

## Tracing the Albian-Cenomanian boundary and OAE1d carbon isotopic excursions in North America: Insights from the Comanche Shelf, northern Gulf of Mexico, USA

Abdulkarim Al-Hussaini <sup>a,b,\*</sup>, Charles Kerans <sup>a,c</sup>, Cornel Olariu <sup>a</sup>, James Pospichal <sup>d</sup>

<sup>a</sup> Department of Earth and Planetary Sciences, Jackson School of Geosciences, The University of Texas at Austin, 2305 Speedway, Stop C1160, Austin, TX 78712-1692, USA

<sup>b</sup> Saudi Aramco, Dhahran 31311, Saudi Arabia

<sup>c</sup> Bureau of Economic Geology, Jackson School of Geosciences, The University of Texas at Austin, 10100 Burnet Rd., Bldg. 130, Austin, TX 78758-4445, USA

<sup>d</sup> BugWare Inc., 1615 Village Square Blvd. Ste 8, Tallahassee, FL 32309, USA

### ARTICLE INFO

Editor: H. Falcon-Lang

**Keywords:**

OAE1d  
Albian-Cenomanian boundary event  
Western Interior Seaway  
Gulf of Mexico  
Comanche Shelf

### ABSTRACT

The late Albian to early Cenomanian time interval experienced significant disturbances in the global carbon cycle, as indicated by notable positive carbon ( $\delta^{13}\text{C}$ ) isotopic excursions (CIEs) that can be traced from the eastern Tethys to the Pacific and Atlantic oceans. Although these positive CIEs are found worldwide, their presence in North America, particularly within the Western Interior Seaway (WIS) and the Gulf of Mexico (GOM), remains insufficiently documented.

Age-constrained  $\delta^{13}\text{C}_{\text{org}}$  data, collected at an approximate vertical sample spacing of 15 cm, combined with detailed sedimentological descriptions from a conventional core taken from the Comanche Shelf of Texas were used to document the sedimentology and carbon isotope stratigraphy of the Albian-Cenomanian boundary for the first time in the WIS and northern GOM margin. These data unveiled the existence of four positive  $\delta^{13}\text{C}_{\text{org}}$  excursions, ranging in magnitude between 0.8 and 1.5 ‰, that are comparable in magnitude and trend to the OAE1d and the other CIEs that dominate this boundary interval worldwide. Additionally, the data presented in this study indicate that the OAE1d interval was primarily characterized by oxic conditions, suggesting a desynchronization between the OAE1d CIE and the deposition of organic-rich sediments on the Comanche Shelf and the southern WIS.

This study offers a comprehensive documentation of the late Albian-early Cenomanian  $\delta^{13}\text{C}$  isotopic excursions in the WIS and northern GOM margin, enabling regional and global correlations with age-equivalent intervals. It highlights parts of the WIS/Comanche Shelf as key sites for further research into the mechanisms that led to regional oxygenation during OAE1d.

### 1. Introduction

The Cretaceous period was marked by significant environmental disruptions that led to the development of multiple oceanic anoxic events (OAEs) on a global scale, characterized by carbon ( $\delta^{13}\text{C}$ ) isotopic excursions (CIEs) and the deposition of widespread organic-rich source rocks (Schlanger and Jenkyns, 1976; Arthur and Schlanger, 1979; Jenkyns et al., 1994; Erba, 2004; Herrele et al., 2004, 2015; Jarvis et al., 2006, 2011; Jenkyns, 2010; Bornemann et al., 2017, 2023; Cramer and Jarvis, 2020). In addition to their importance in developing

hydrocarbon source rocks, these OAEs have been widely used to explain global carbonate factory demise (Arthur and Schlanger, 1979; Schlager, 1981; Hallock and Schlager, 1986; Philip and Airaud-Crumiere, 1991; Phelps et al., 2015), serving as reliable time markers for global correlation. A particularly important interval within the Cretaceous period is the Albian-Cenomanian boundary, where notable carbon isotopic excursions indicate shifts in the global carbon cycle (Gale et al., 1996; Vahrenkamp, 2013; Jarvis et al., 2006; Wohlwend et al., 2016; Bornemann et al., 2017; Yao et al., 2018; Cramer and Jarvis, 2020).

The late Albian oceanic anoxic event (OAE1d- Breistroffer Event)

\* Corresponding author at: Department of Earth and Planetary Sciences, Jackson School of Geosciences, The University of Texas at Austin, 2305 Speedway, Stop C1160, Austin, TX 78712-1692, USA.

E-mail address: [abdulkarim.alhussaini@gmail.com](mailto:abdulkarim.alhussaini@gmail.com) (A. Al-Hussaini).

was first recognized as a local paleoclimatic event within the Vocontian Trough of southeast France, associated with the deposition of organic-rich mudstones (Breistroffer, 1937; Bréhéret, 1988, 1997; Gale et al., 1996; Bornemann et al., 2005). Detailed geochemical studies from the Vocontian Trough have revealed that the OAE1d is one of four significant  $\delta^{13}\text{C}$  positive excursions (lettered from base to top; A-D) dominating the Albian-Cenomanian boundary (Gale et al., 1996; Kennedy et al., 2004; Bornemann et al., 2005). Following their discovery in France, the late Albian-early Cenomanian  $\delta^{13}\text{C}$  excursions (including the OAE1d) were fully or partially reported from the Tethys Ocean (e.g., Vahrenkamp, 2013; Gambacorta et al., 2015, 2020; Wohlwend et al., 2016; Gyawali et al., 2017; Yao et al., 2018; Hennhoefer et al., 2019; Navidtalab et al., 2019), Boreal Ocean (Mitchell et al., 1996; Jarvis et al., 2006; Bornemann et al., 2017, 2023), Atlantic Ocean (Wilson and Norris, 2001; Nederbragt et al., 2001; Petrizzo et al., 2008), South

America (Navarro-Ramirez et al., 2017; Rodríguez-Cuicas et al., 2019, 2020), and the Pacific Ocean (Robinson et al., 2008; Navarro-Ramirez et al., 2015).

While the four late Albian-early Cenomanian  $\delta^{13}\text{C}$  excursions indicate detectable disturbances in the global carbon cycle that can be traced from the eastern Tethys to the Pacific and Atlantic oceans, a stratigraphically complete record of these events on the North American Plate, specifically within the WIS and GOM, has not yet been comprehensively documented. Recently, several studies have significantly advanced the understanding of the Albian-Cenomanian carbon isotope stratigraphy in North America. For instance, high-resolution  $\delta^{13}\text{C}$  and  $p\text{CO}_2$  records provided by Gröcke et al. (2006) and Richey et al. (2018) have documented key segments of the OAE1d excursion in the Rose Creek pit of Nebraska. Schröder-Adams et al. (2012), Scott et al. (2013, 2019), and Phelps et al. (2015) provided valuable  $\delta^{13}\text{C}$  profiles that hint

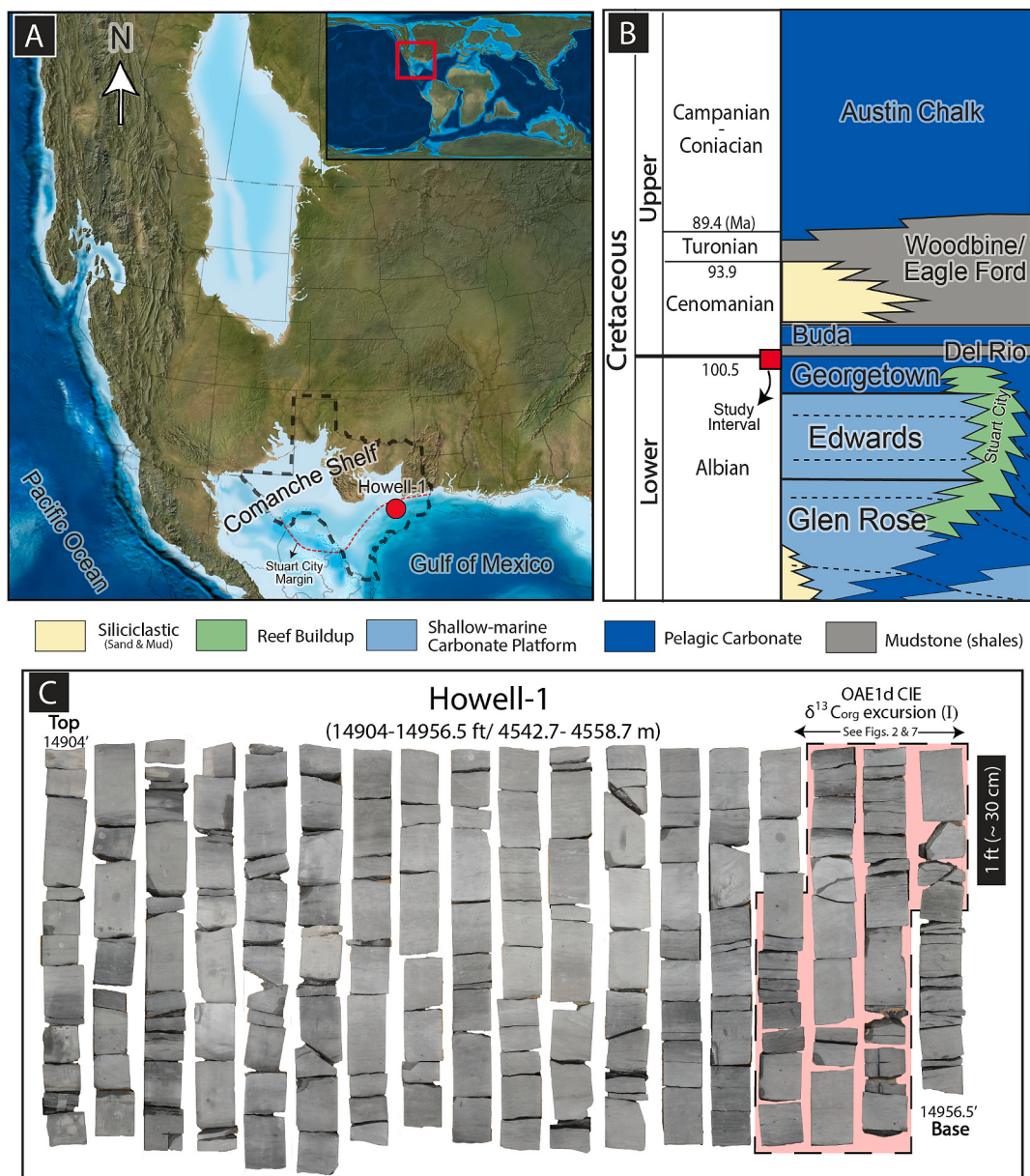


**Fig. 1.** (A) A paleogeographic map of the southern Western Interior Seaway/Comanche Shelf and the Gulf of Mexico during the late Albian time illustrating the location of the Howell-1 well (Source: Colorado Plateau Geosystem Inc., UT library). (B) A generalized stratigraphic column for parts of the Cretaceous stratigraphy of Texas describing the dominant lithologies of the interval from the Glen Rose to Austin Chalk formations (modified after Phelps et al., 2014). The study interval (Albian-Cenomanian Boundary) is highlighted by the red square. (C) Plan-view core photograph of the Howell-1 core used in this study, with a highlight of the OAE1d CIE interval. (For interpretation of the references to colour in this figure legend, the reader is referred to the web version of this article.)

at the potential presence of the late Albian–early Cenomanian isotopic excursions in the WIS-GOM region, though these records remain partially constrained by factors such as limited sampling resolution, diagenetic overprinting, and/or stratigraphic incompleteness. Collectively, these studies lay a critical foundation for ongoing research, highlighting both the potential for these isotopic events to be recorded within the interior of North America and the necessity for more continuous, high-resolution  $\delta^{13}\text{C}$  records.

Building on prior work in the region, this study aims to explore the sedimentology and carbon isotope stratigraphy of the late Albian–early Cenomanian interval in the WIS and northern GOM margin, utilizing subsurface data from the Comanche Shelf of Texas. It focuses on providing a high-resolution and stratigraphically complete documentation of the OAE1d and the three overlying CIEs within this interval from the Comanche Shelf, linking North America with age-equivalent intervals from the adjacent Pacific and Atlantic oceans, as well as other basins across the globe. Moreover, this study provides a basis for reassessing the current paleoceanographic understanding of North America.

## 2. Geological settings and stratigraphy

Due to the Mesozoic breakup of Pangea, the North American Plate was detached from the South American and African plates, leading to the formation of the GOM Basin (Buffler, 1991; Ewing, 1991; Salvador, 1991; Snedden and Galloway, 2019). The Comanche Shelf and the Stuart City margin, rimming the northern GOM, represent a vast continental shelf that linked the shallow water of the WIS with the GOM deepwater during most of the Albian stage (Fig. 1A) (Salvador, 1991; Snedden and Galloway, 2019).

During most of the Albian, the Comanche Shelf was dominated by shallow-water interior platform carbonates transitioning seaward into a NE-SW oriented rudist-dominated shelf margin commonly referred to as the Stuart City margin (Rose, 1972; Kerans, 2002; Waite et al., 2007; Phelps et al., 2014). Towards the late Albian–early Cenomanian, the Comanche Shelf of Texas and its rudist-dominated rimmed margin (Stuart City) were flooded and covered by the mud-dominated carbonates and clay-rich mudstones of the Georgetown and Del-Rio formations, respectively (Fig. 1B) (Kerans, 2002; Phelps et al., 2014; Scott et al., 2019). Several biostratigraphic studies indicate that the Albian–Cenomanian boundary is near the contact between the Georgetown carbonates and the overlying Del-Rio mudstones (Mancini, 1979; Scott et al., 2003, 2018).

## 3. Dataset and methodology

The dataset for this study derives from one continuous core with a total thickness of ~16 m (52.5 ft) from the Humbel Howell-1 well (30° 46' 13.0" N, 94° 29' 29.8" W) in Taylor County, Texas (Fig. 1), encompassing the Albian–Cenomanian boundary. A detailed core description was performed to define major lithofacies and stratigraphic contacts. In addition to the core description, samples were taken for thin section petrography, organic carbon isotopic, total organic carbon (TOC), and nannofossil analyses.

### 3.1. Carbon isotope and TOC analyses

A total of 104 samples were collected for organic carbon ( $\delta^{13}\text{C}_{\text{org}}$ ) isotope analysis using a hand-held drill, with an approximate vertical sample spacing of 15 cm. The analysis of  $\delta^{13}\text{C}_{\text{org}}$  was selected to accurately capture the primary carbon isotope signals related to marine productivity and organic carbon burial. This approach, which aims to minimize the impact of diagenetic alteration that often affects bulk carbonate  $\delta^{13}\text{C}$  values (e.g., Allan and Matthews, 1990; Dickson and Coleman, 1990), builds on findings from previous studies in Texas (e.g., Phelps et al., 2015; Scott et al., 2019) that identified some diagenetic overprinting across their Albian–Cenomanian  $\delta^{13}\text{C}$  records.

Approximately 25–30 mg of powdered material were extracted from each of the 104 collected samples and placed into 6 × 4 mm silver capsules to be used for the  $\delta^{13}\text{C}_{\text{org}}$  and TOC analyses. Three rounds of acid fumigation utilizing 4 N HCl at 65 °C were applied to the collected samples within the silver capsules to separate the organic carbon. The  $\delta^{13}\text{C}_{\text{org}}$  and TOC analyses were measured using a Costech 4010 Elemental Analyzer combustion system (at 1060 °C) and a Thermo DeltaV Plus Isotopic Ratio Mass Spectrometer. The  $\delta^{13}\text{C}_{\text{org}}$  and TOC values are reported in per mil (‰) relative to the Vienna Pee Dee Belemnite (VPDB) standard and in weight percent (wt%), respectively. The  $\delta^{13}\text{C}_{\text{org}}$  measurements were calibrated using international reference materials, including IAEA-CH-3 (cellulose) from the International Atomic Energy Agency, USGS-24 (graphite) from the United States Geological Survey, Casein Protein and Urea from Elemental Micro-analysis. Measured values for these standards yielded standard deviations ranging from 0.05 ‰ to 0.10 ‰, indicating a  $\delta^{13}\text{C}_{\text{org}}$  reproducibility better than ±0.1 ‰.

### 3.2. Nannofossil analysis and thin section petrography

Fourteen samples were retrieved from the Howell-1 core for nannofossil analysis and thin section petrography, with seven samples designated for each. The petrographic sampling targeted facies variations, while the nannofossil sampling primarily focused on the argillaceous intervals to ensure better nannofossil recovery for age dating (Fig. 2).

For nannofossil analysis, the seven core samples were analyzed using smear slides prepared by standard methods (see Bown, 1998). Slides were examined using an Olympus BX53 petrographic microscope, based on 100 fields of view at 1200× magnification, and photographs of key nannofossil specimens were taken with a PAXcam 5 digital camera. The biostratigraphic zonations of Bown et al. (1998) and Burnett (1998) were applied.

## 4. Results

### 4.1. Lithofacies

The described core from the Howell-1 well (between 14,904' to 14,956.5' ft./ 4542.7 to 4558.7 m) is dominated by calcisphere-foraminiferal (*Globigerina* spp.) wackestone/packstone, exhibiting very subtle facies variations (Fig. 2). The uppermost 3 m (~10 ft) interval shows more argillaceous content in addition to thin layers (~3 to 15 cm) of clay-rich mudstone (Figs. 2 & 3). Bioturbation is common throughout the core, with intensities ranging between 0 and 4 on the bioturbation index (BI) of Taylor and Goldring (1993). *Planolites*, *Asterosoma*, *Nereites*, *Zoophycos*, *Ophiomorpha*, and *Schaubcylindrichnus* are the most common trace fossils identified within the analyzed interval. Unlike the outcrops in North Texas, where a stratigraphic discontinuity at the Albian–Cenomanian boundary is assumed based on the presence of hardground surfaces (Scott et al., 2019; Gale et al., 2021), the Howell-1 core exhibits a homogenous interval with no evidence of a break in sedimentation (Fig. 1C). A detailed description of the facies encountered within the Howell-1 core is summarized in Table 1.

### 4.2. Nannofossil biostratigraphy

Nannofossil abundance in samples examined is generally high, ranging between 800 and 5000 (based on 100 fields of view at 1200 X magnification). Preservation is mostly moderate with minor calcite overgrowth or in some cases, etching and fragmentation. The samples yielded the following stratigraphically important species: *Eiffellithus hancockii*, *E. parvus*, *E. equibiramus*, *E. turrieseiffelii*, *E. paragogus*, *Ellipsogelosphaera britannica*, *Gartnerago gammation*, *Nannoconus fragilis*, *Zeugrhabdotus xenotus*, *G. stenostaurion*, *Lithraphidites alatus* (Fig. 4 and Supplementary Data). *Hayesites albiensis* and *Corollithion kennedyi* were

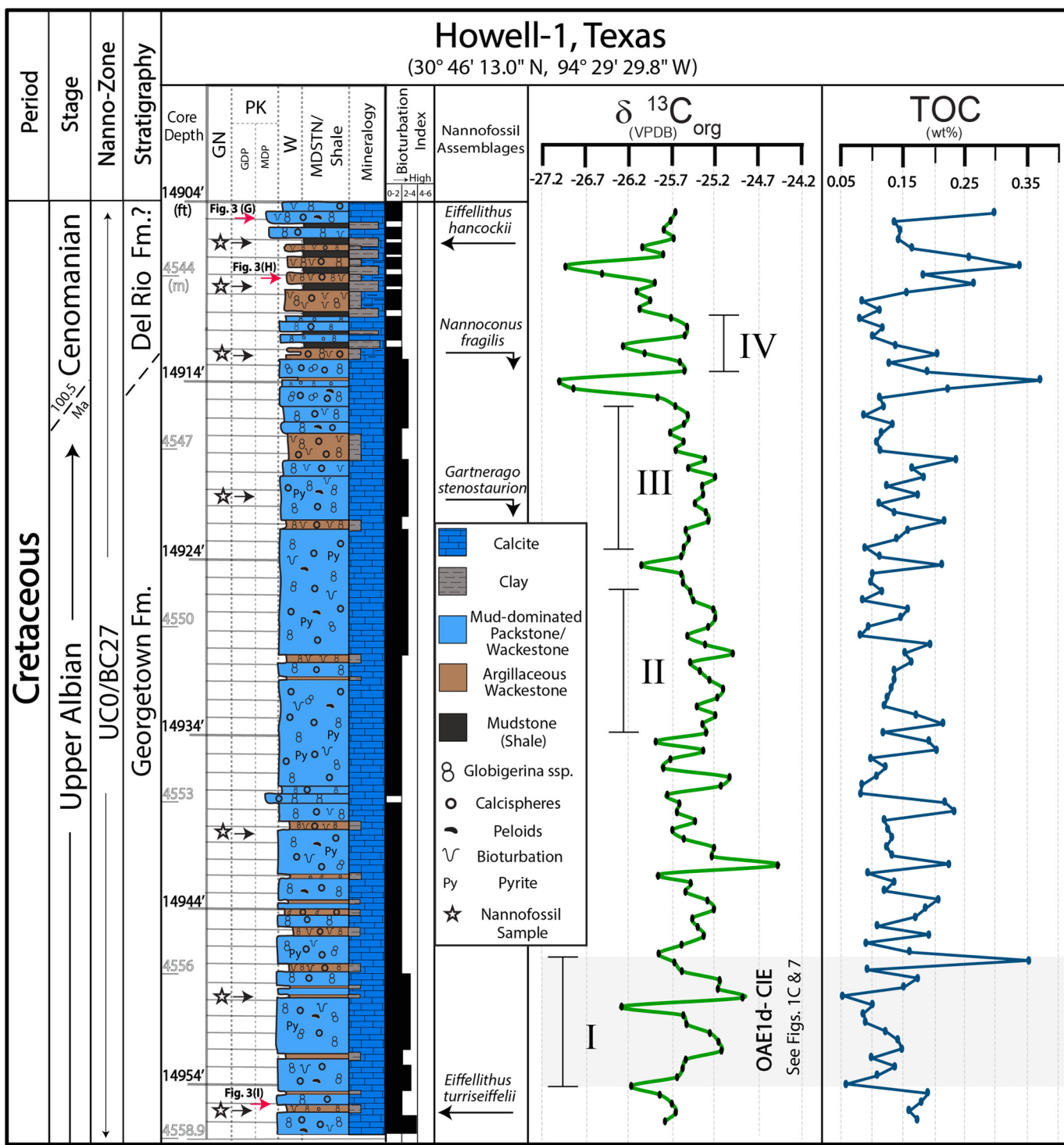


**Fig. 2.** A detailed core description profile for the Howell-1 alongside the  $\delta^{13}\text{C}_{\text{org}}$  data and the stratigraphic positions of some age-diagnostic nannofossils. Intervals I through IV highlight the four positive  $\delta^{13}\text{C}_{\text{org}}$  excursions encountered within the Howell-1 core. Please refer to Figs. 6 and 7 for detailed information about the correlation of the OAE1d-CIE from Howell-1 with other OAE1d CIEs documented globally. MDSTN: Mudstone, W: Wackestone, PK: Packstone, MDP: Mud-dominated Packstone, GDP: Grain-dominated Packstone, GN: Grainstone.

not noted in the Howell-1 samples.

The abovementioned nannofossil species are commonly reported from the late Albian-early Cenomanian interval of many basins around the globe (e.g., Jeremiah, 1996; Bown, 1998; Burnett, 1998; Bown, 2005; Watkins et al., 2005; Hennhofer et al., 2019; Kanungo et al., 2021), including the global boundary stratotype section and point (GSSP) in France (Gale et al., 1996; Kennedy et al., 2004) (Fig. 5). The

last occurrence of *Nannoconus fragilis* and *Gartnerago stenostaurion* (at 14912.25'/4545.25 m and 14,920.5'/4547.75 m, respectively; Fig. 4G & 4L-N) suggest an uppermost Albian age transitioning into Cenomanian (cf. Perch-Nielsen, 1985; Gale et al., 1996; Kennedy et al., 2004; Kanungo et al., 2021; Alves et al., 2024) (Fig. 5).

Based on the identified nannofossil assemblages, the Howell-1 core is placed within the BC27/UCO zone of Burnett (1998) between the last

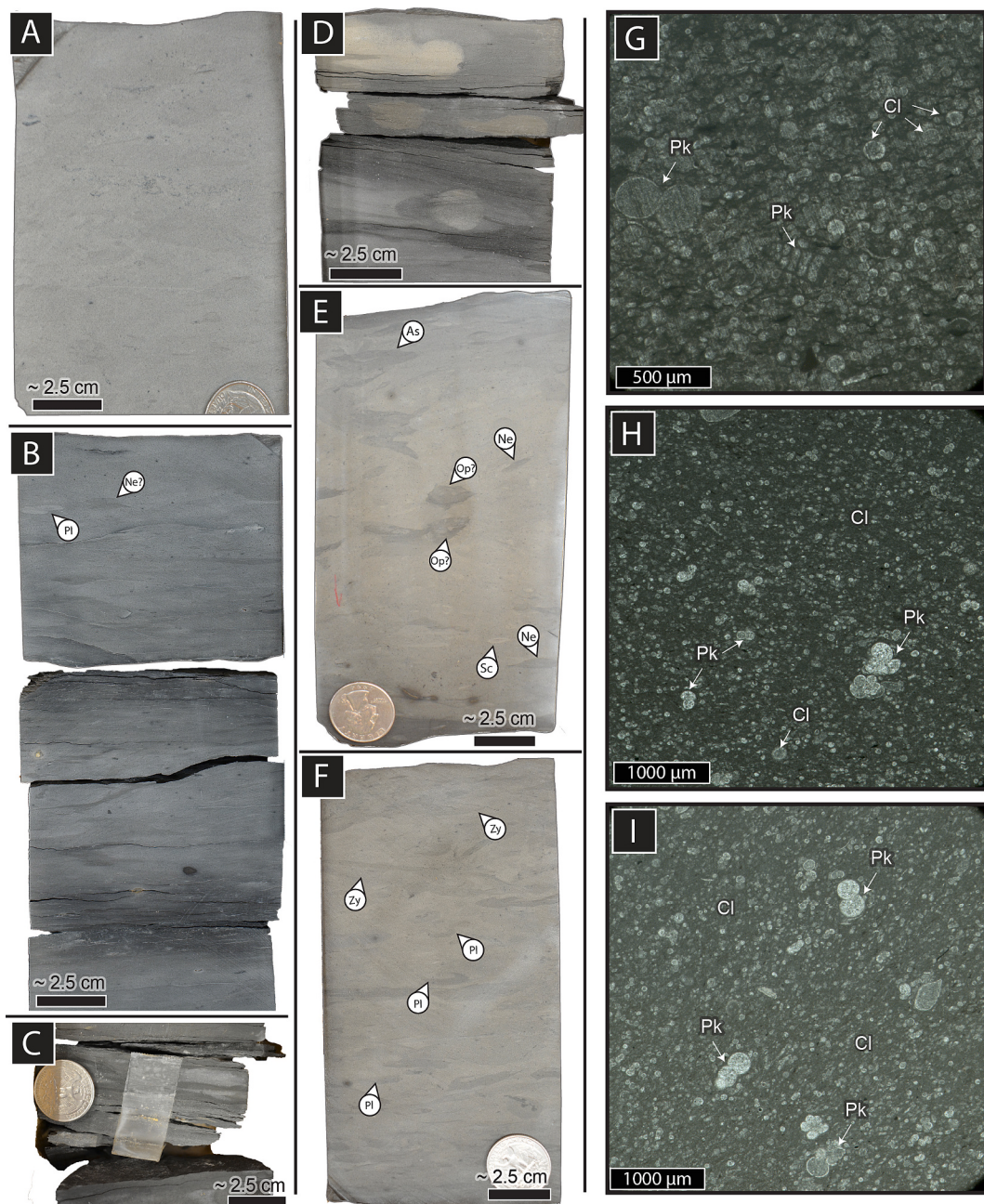


**Fig. 3.** Core and thin-section photographs from the Howell-1 core. (A–B) Core photographs for the calcisphere-foraminiferal MDP/wackestone (F1) and the argilaceous calcisphere-foraminiferal wackestone (F2), respectively. (C–D) Core photographs for the clay-rich mudstones (F3). (E–F) Close-up core photographs indicating some of the observed trace fossils (As: *Asterosoma*, Zy: *Zoophycos*, Pl: *Planolites*, Ne: *Nereites*, Op: *Ophiomorpha*, Sc: *Schaubcyclindrichnus*) within the Howell-1 core. (G–I) Thin-section photographs illustrating the main constituent grains (Pk: Planktonic foraminifera, Cl: Calcisphere) observed within the Howell-1 core.

occurrence of *Hayesites albiensis* and the first occurrence of *Corollithion kennedyi* and the upper range of *Ellipsagelosphaera britannica* (Fig. 5).

#### 4.3. Carbon isotope and total organic carbon (TOC) trends

The  $\delta^{13}\text{C}_{\text{org}}$  measurements from the Howell-1 core range from  $-27.1$  to  $24.5\text{ ‰}$ , illustrating four positive excursions that are separated by negative excursions of  $0.7$  to  $1.5\text{ ‰}$ . The four positive  $\delta^{13}\text{C}_{\text{org}}$  excursions range in magnitude from  $0.8$  to  $1.5\text{ ‰}$  and are labeled from base to top as I through IV (Fig. 2 and Supplementary Data). Among the four positive  $\delta^{13}\text{C}_{\text{org}}$  excursions, the first (I) and fourth (IV) display the largest magnitude of  $1.3$  and  $1.5\text{ ‰}$ , respectively. In contrast, the second (II) and third (III) excursions display lower values, at  $0.9$  and  $0.8\text{ ‰}$ ,

respectively.

The TOC values from the Howell-1 core are very low, ranging between  $0.05$  and  $0.37\text{ wt\%}$ , with no major enrichment across the abovementioned positive  $\delta^{13}\text{C}_{\text{org}}$  excursions (Fig. 2). A slight increase in TOC, reaching up to  $0.37\text{ wt\%}$ , is observed towards the top of the Howell-1 core, closely associated with the thin layers of the clay-rich mudstone.

**Table 1**

Summary of the identified lithofacies within the Howell-1 core.

Facies	Description	Constituent Grains	Thickness (m)	Bioturbation Intensity (BI)
F1: Calcisphere- Foraminiferal Mud-dominated Packstone to Wackestone	Grey to light grey mud-dominated packstone to wackestone, contains few pyrite nodules and peloids	Calcspheres and planktonic foraminifera ( <i>Globigerina</i> ssp.?)	~ 0.15–1.8	None to moderate (BI ~ 0–4) <i>Planolites</i> , <i>Asterosoma</i> , <i>Zoophycos</i> , <i>Nereites</i> , <i>Ophiomorpha</i> , <i>Schaubcylindrichnus</i>
F2: Argillaceous, Calcisphere-Foraminiferal Wackestone	Dark grey to grey wackestones, commonly interbedded with mm-scale dark grey argillaceous laminations	Calcspheres and planktonic foraminifera ( <i>Globigerina</i> ssp.?)	~ 0.05–0.38	Low (BI ~ 1–2) <i>Planolites</i> and undifferentiated burrows ( <i>Nereites</i> ?)
F3: Clay-rich mudstone	Dark grey to blackish grey clay-rich mudstones that display some fissility in parts	–	~ 0.03–0.15	No obvious bioturbation

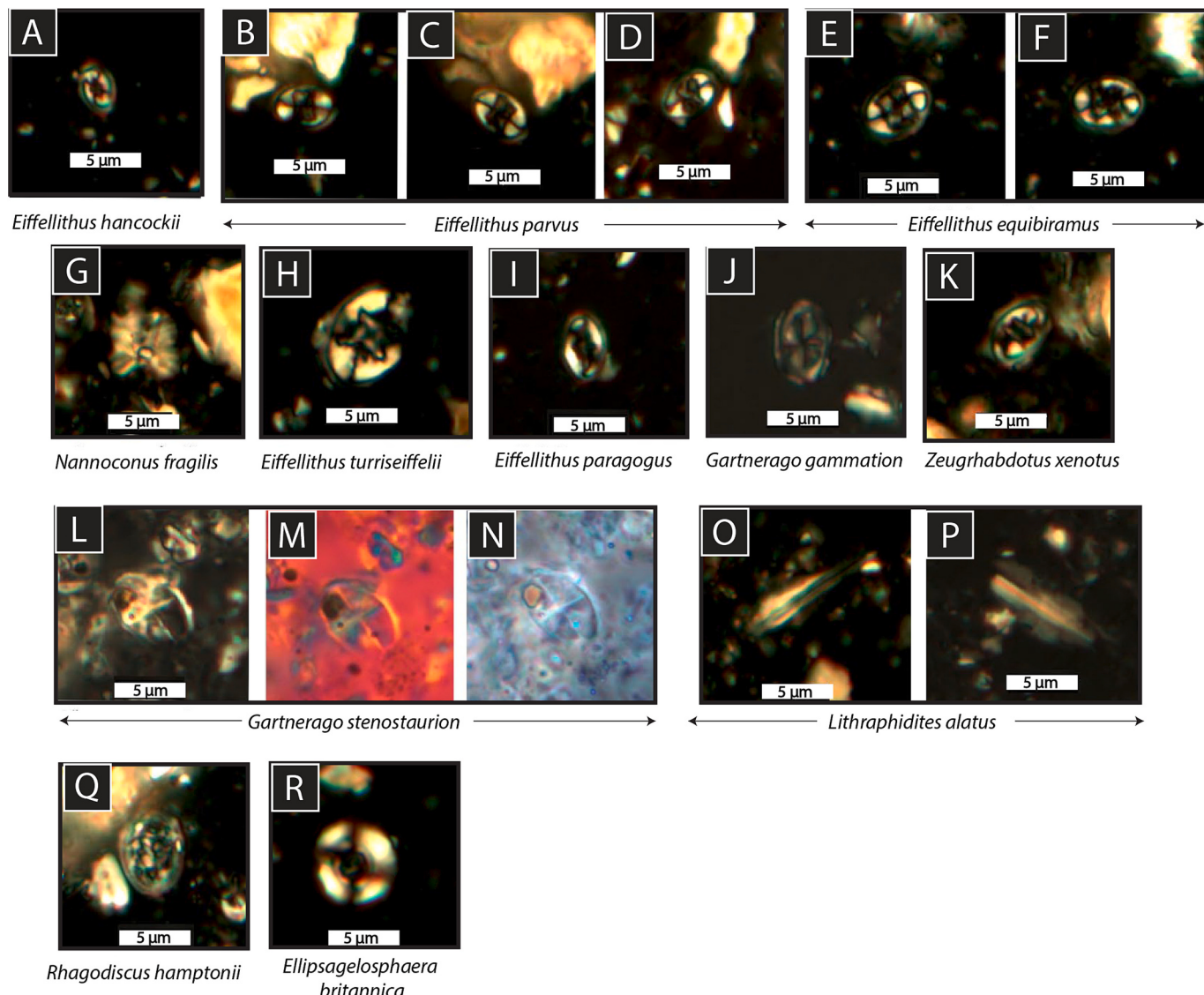


**Fig. 4.** Photographs of representative nannofossil assemblages from the Howell-1 core samples. (A) *Eiffellithus hancockii*, (B–D) *Eiffellithus parvus*, (E–F) *Eiffellithus equibiramus*, (G) *Nannoconus fragilis*, (H) *Eiffellithus turriseiffelii*, (I) *Eiffellithus paragogus*, (J) *Gartnerago gammation*, (K) *Zeugrhabdotus xenotus*, (L–N) *Gartnerago stenostaurion* (XPL, gypsum plate and PPL, respectively), (O–P) *Lithraphidites alatus*, (Q) *Rhagodiscus hamptonii*, (R) *Ellipsagelosphaera britannica*.

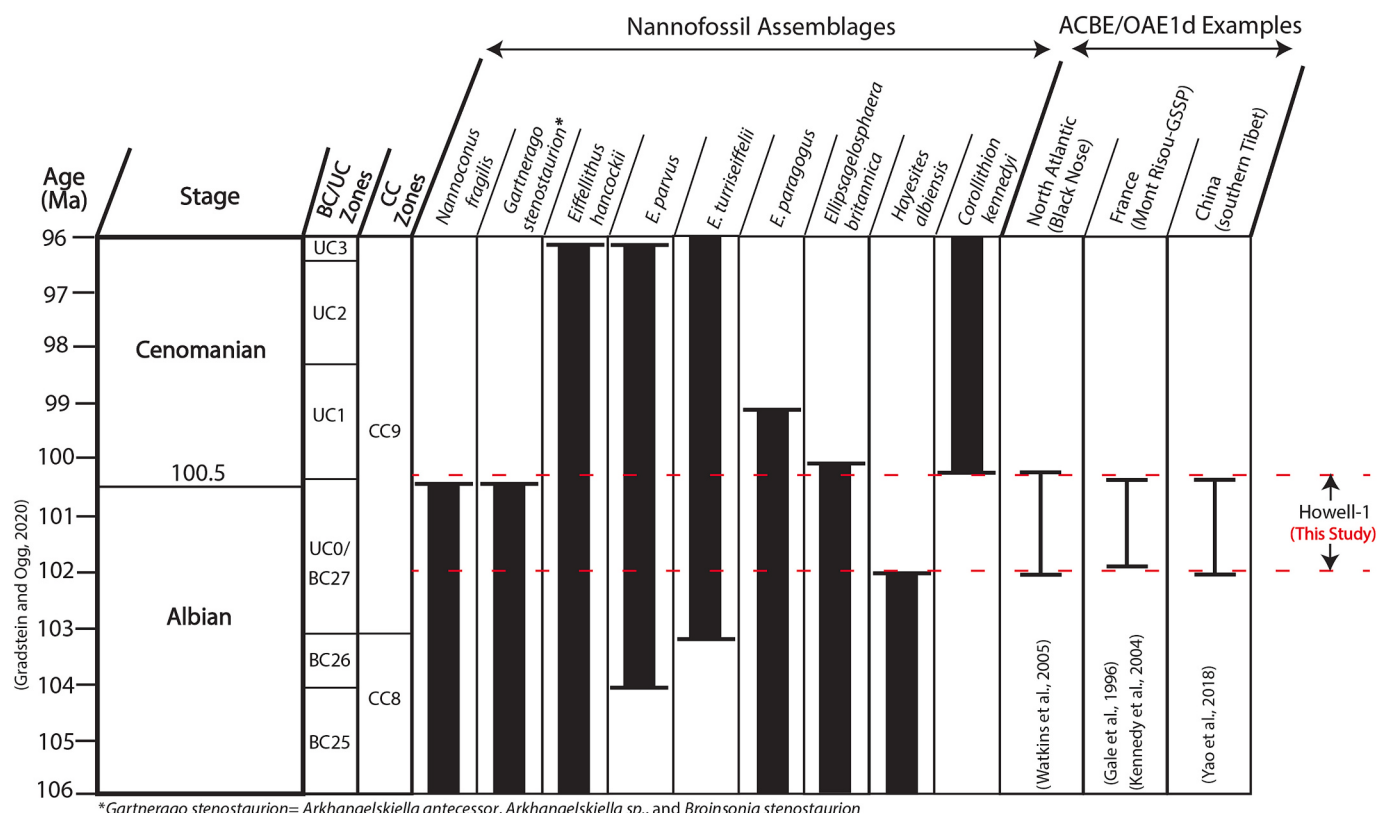


**Fig. 5.** Detailed representation of the stratigraphic ranges of certain Cretaceous nannofossil assemblages that are commonly reported from stratigraphic sections spanning the Albian-Cenomanian Boundary (ACBE), along with a comparison between the stratigraphic position of Howell-1 and other Albian-Cenomanian sections from the North Atlantic (Watkins et al., 2005), France (Gale et al., 1996; Kennedy et al., 2004), and China (Yao et al., 2018). The represented stratigraphic ranges for the nine nannofossil assemblages presented in this figure were obtained from Perch-Nielsen (1985), Gale et al. (1996), Jeremiah (1996), Bown et al. (1998), Burnett (1998), Kennedy et al. (2004), Bown (2005), Watkins et al. (2005), Kanungo et al. (2021), and Alves et al. (2024). Geological ages and their correlation with nannofossil zonations were retrieved from (Gale et al., 2020; Gradstein and Ogg, 2020). The red dashed lines indicate the last occurrence of *Hayesites albiensis* and the first occurrence of *Corollithion kennedyi*. Detailed counting of the Howell-1 nannofossils can be found in the supplementary file. (For interpretation of the references to colour in this figure legend, the reader is referred to the web version of this article.)

## 5. Discussion

### 5.1. First complete carbon isotope record of the Albian-Cenomanian boundary and OAE1d in the Western Interior Seaway (WIS) and Gulf of Mexico (GOM)

Despite their long-known existence within many basins worldwide, including the nearby Atlantic and Pacific oceans, a complete record of the four late Albian-early Cenomanian  $\delta^{13}\text{C}$  isotopic excursions (with OAE1d as the lowermost excursion) on the North American Plate remains unconstrained. At the Rose Creek pit in Nebraska, high-resolution terrestrial  $\delta^{13}\text{C}_{\text{org}}$  and  $p\text{CO}_2$  records from an Albian-Cenomanian fluvial-estuarine succession captured segments of the OAE1d excursion, interrupted by a potential depositional hiatus (Gröcke et al., 2006; Richey et al., 2018). In the Western Canada Sedimentary Basin, a positive  $\delta^{13}\text{C}$  excursion (~1.0‰) is interpreted to represent the OAE1d, but erosion attributed to forebulge-related tectonism has removed much of the uppermost Albian succession (Schröder-Adams et al., 2012), leaving no record of the other three overlying  $\delta^{13}\text{C}$  excursions. Within the Mesilla Valley Formation of the Chihuahua Trough in New Mexico, Scott et al. (2013) tentatively identified the OAE1d interval by recognizing a +1.6‰  $\delta^{13}\text{C}_{\text{org}}$  excursion across Fe-enriched mudstone with TOC values ranging between 0.25 and 0.69 wt%; however, the authors explicitly noted that their coarse sampling resolution (~2–5 m sampling interval) limited confidence in fully capturing the isotopic and geochemical expression of the OAE1d in this region. Across Texas, both Phelps et al. (2015) and Scott et al. (2019) provided  $\delta^{13}\text{C}_{\text{carb}}$  data spanning the

Albian-Cenomanian boundary but documented no expression of the OAE1d or other CIEs, attributing their absence to various possible factors such as low sampling resolution, stratigraphic discontinuities, diagenetic overprinting, and/or limited regional development. As a whole, these previous studies have laid a strong foundation for understanding this interval in the WIS-GOM region by defining key limitations and highlighting valuable research opportunities to strengthen global correlations between North America and age-equivalent intervals elsewhere.

In this context, the present study fills a critical knowledge gap by providing a continuous  $\delta^{13}\text{C}_{\text{org}}$  record that captures all the four globally recognized late Albian–early Cenomanian isotopic excursions within the WIS-GOM region. The nannofossil assemblages in the Howell-1 core place the studied interval as time-equivalent to the GSSP in France, where the four CIEs (lettered A-D) were first defined (Gale et al., 1996) (Figs. 4 & 5). The four (I through IV) positive  $\delta^{13}\text{C}_{\text{org}}$  excursions observed in the Howell-1 well of Texas display similarity with the four  $\delta^{13}\text{C}$  isotopic excursions (A-D) reported from the Mont Risou (GSSP) section in France (Gale et al., 1996), DSDP Site 547 in the North Atlantic Ocean (Nederbragt et al., 2001), the Permanente Quarry of California in the paleo-Pacific Ocean (Robinson et al., 2008), the Lower Saxony Basin of Germany (Bornemann et al., 2017), Jabal Qusaybah & Jabal Madamar in Oman (Wohlwend et al., 2016), and the southern Tibet in China (Yao et al., 2018) (Fig. 6).

The lowermost positive  $\delta^{13}\text{C}_{\text{org}}$  excursion (I) in Howell-1, falling entirely within the late Albian, exhibits a magnitude of 1.3‰ (Figs. 6 & 7). Based on correlation with age-equivalent intervals, our first (I)

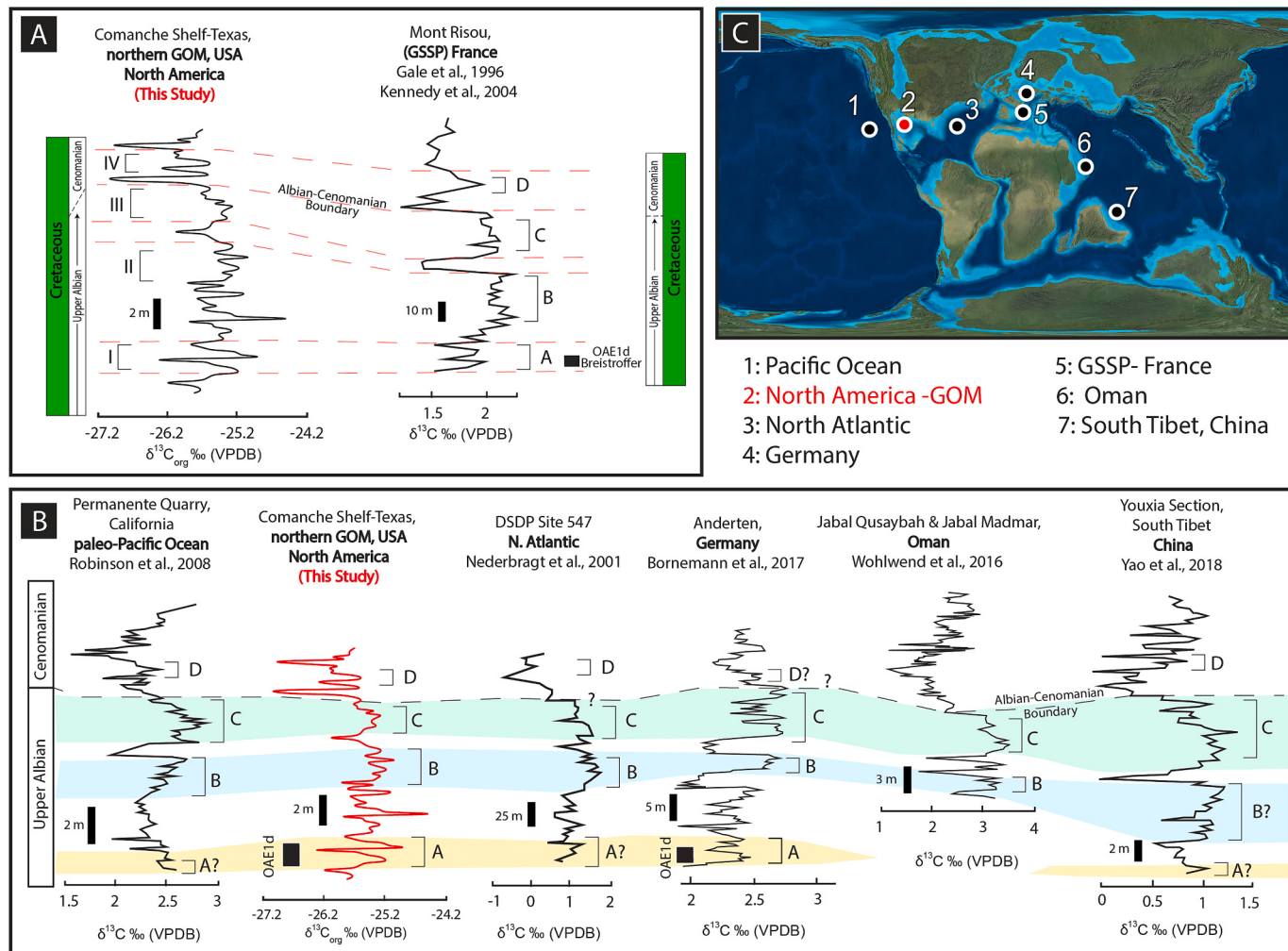


**Fig. 6.** (A) δ<sup>13</sup>C correlation between the Howell-1 well and the GSSP in France (Gale et al., 1996; Kennedy et al., 2004). (B) δ<sup>13</sup>C correlation between the Howell-1 well and other localities worldwide: Pacific Ocean (Robinson et al., 2008), North Atlantic (Nederbragt et al., 2001), Germany (Bornemann et al., 2017), Oman (Wohlwend et al., 2016), China (Yao et al., 2018). (C) A global paleogeographic map of the late Albian stage illustrating the localities presented in (B) (Source: Colorado Plateau Geosystem Inc., UT library).

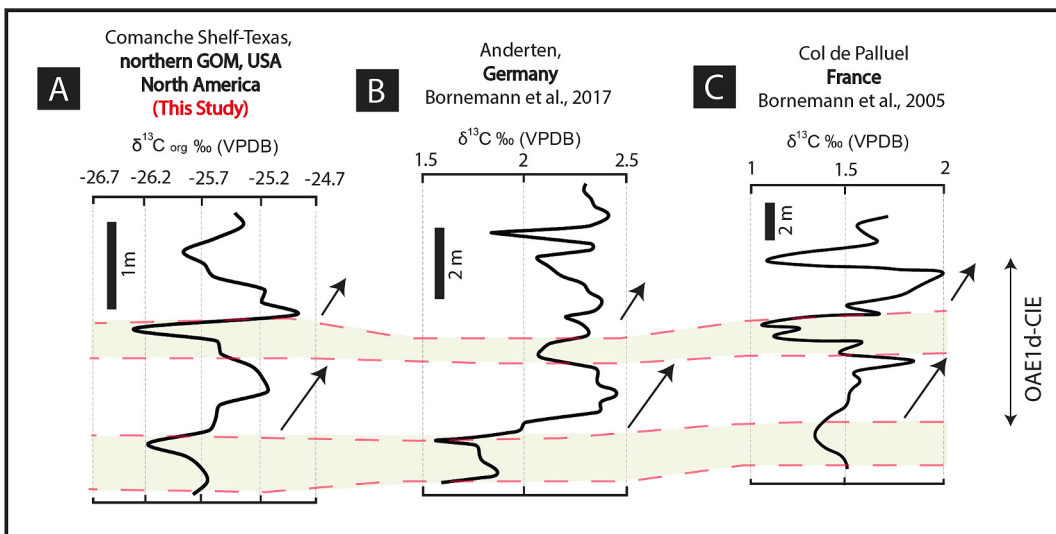


**Fig. 7.** Close-up δ<sup>13</sup>C correlation between (A) the OAE1d CIE reported in this study from the Comanche Shelf of Texas and other OAE1d CIEs from (B) the Anderten Basin in Germany (Bornemann et al., 2017) and (C) Col de Palluel in France (Bornemann et al., 2005).

positive excursion exhibits a similar trend and magnitude to the  $\delta^{13}\text{C}$  excursion recorded globally during the OAE1d/Breistroffer event, which ranges from 0.5 ‰ to 2.0 ‰ (e.g., Gale et al., 1996; Gröcke et al., 2006; Bornemann et al., 2005, 2017; references therein) (Fig. 7). Towards the top of Howell-1 core, close to where the nannofossil age dating of this study places the Albian-Cenomanian boundary, a noticeable negative  $\delta^{13}\text{C}_{\text{org}}$  excursion (~ 2.0 ‰), associated with slight increase in TOC, is observed between the third (III) and fourth (IV) positive isotope excursions. This excursion is akin to the negative  $\delta^{13}\text{C}$  excursion reported near the Albian-Cenomanian boundary between the “C” and “D” isotopic peaks from different places around the world (Fig. 6) (e.g., Gale et al., 1996; Wohlwend et al., 2016; Yao et al., 2018). Overall, the  $\delta^{13}\text{C}_{\text{org}}$  excursions of Howell-1 are similar in magnitude to those observed globally; however, they are more closely aligned with data from the nearby Pacific and Atlantic regions than those from the Tethyan and Boreal realms (Fig. 6). This stronger connection between Howell-1 and the Pacific and Atlantic data suggests that these areas may have

experienced similar regional oceanographic conditions.

To the best of our knowledge, the presented age-constrained  $\delta^{13}\text{C}_{\text{org}}$  data from Howell-1 represent the first complete documentation of the four globally mapped Albian-Cenomanian isotopic excursions in the WIS-GOM region. The findings of this study provide a new data point that can aid in linking the Albian-Cenomanian interval of North America with age-equivalent intervals from the nearby Pacific and Atlantic oceans, as well as globally.

### 5.2. Decoupling between the OAE1d CIE and the development of organic-rich mudstones

Oceanic Anoxic Events (OAEs) are often associated with significant environmental changes, leading to notable CIEs and the deposition of widespread organic-rich source rocks due to prevailing anoxic conditions (Jenkyns, 2010; Cramer and Jarvis, 2020; references therein). Nevertheless, recent studies have indicated that there can be instances

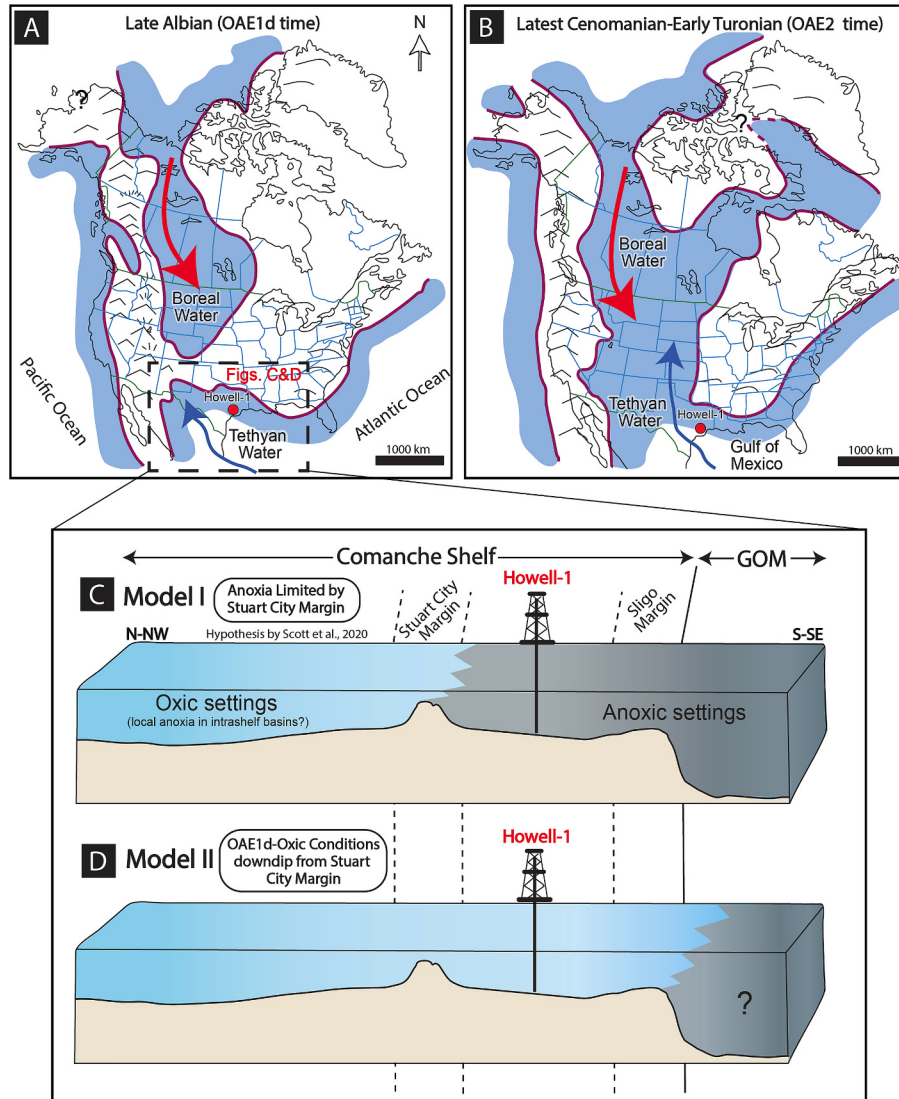


**Fig. 8.** (A) Late Albian and (B) Latest Cenomanian-Early Turonian paleogeographic maps of North America illustrating that the southern and northern parts of the Western Interior Seaway were not connected till the OAE2 time, suggesting almost no mixing between the Tethyan and Boreal waters during the OAE1d. Both maps were modified after Schröder-Adams et al. (2012). See Williams and Stelck (1975), Cobban et al. (1994), Roberts and Kirschbaum (1995) for more details on the paleogeographic reconstruction of the WIS during the Albian-Cenomanian interval. (C & D) Two models explaining the lateral extent of the OAE1d anoxic settings into the Comanche Shelf. (C) The Stuart City margin was acting as a bathymetric sill limiting anoxic conditions to areas south of the Stuart City margin besides some possible localized anoxia in up-dip intrashelf basins (model hypothesized by Scott et al., 2020). (D) Oxic settings prevailed in the areas between the Stuart City and Sligo margins (this study).

where decoupling between CIEs and the deposition of organic-rich sediments may occur during well-defined OAEs, such as the Jurassic Toarcian OAE (T-OAE) and the Cenomanian-Turonian boundary event (OAE2) (Eldrett et al., 2014; Alnazgah et al., 2022; Herlambang et al., 2023; Ge et al., 2024; references therein).

A prominent example of this decoupling phenomenon has been documented from parts of the Comanche Shelf and the WIS, where the OAE2 CIE coincided with elevated oxygen levels and low TOC content (e.g., Pratt and Threlkeld, 1984; Leckie, 1985; Leckie et al., 1998; Elderbak et al., 2014; Eldrett et al., 2014; Denne et al., 2016). Overall, there is general agreement in the literature that the oxygenation of the WIS during the OAE2 was driven by the mixing of the Tethyan and Boreal water masses during periods of relative sea-level rise (Fig. 8A & B) (Elderbak and Leckie, 2016; Eldrett et al., 2017; Lowery et al., 2018; references therein).

The OAE1d CIE interval in the Howell-1 core (14,946–14,954'/4555.5–4558 m) coincides with bioturbated pelagic carbonates, indicating adequate bottom-water oxygenation (Figs. 1C & 2). Additionally, the very low TOC values (<0.35 wt%) across the OAE1d CIE in the Howell-1 further support the interpretation of oxic conditions on the Comanche Shelf and southern WIS during the OAE1d/Breistroffer interval (Fig. 2). This trend differs from the OAE1d expression in many basins around the world, where the OAE1d CIE was found to be associated with the deposition of organic-rich sediments (e.g., Gale et al., 1996; Bornemann et al., 2005; Petrizzo et al., 2008; Gambacorta et al., 2020; Bak et al., 2023). However, it is consistent with examples of CIE-TOC decoupling reported from the Arabian Plate, such as the Natih Formation in Oman and the Shilaif Basin in the United Arab Emirates, where the OAE1d CIE occurs below or above the main organic-rich intervals (Vahrenkamp, 2013; Hennhoefer et al., 2019). These cases support the variability in how the OAE1d was expressed across different basins, highlighting the need for further research to better constrain the mechanisms driving these differences.

The OAE1d decoupling in Howell-1 reflects a regional pattern similar to the decoupling trend observed during the OAE2 on parts of the Comanche Shelf and WIS, proposing some persistent local controls. Although it is beyond the scope of this study to investigate the root cause of this decoupling phenomenon on the Comanche Shelf and WIS, the extent of this trend to the underlying OAE1d, as indicated by the Howell-1 data, necessitates a review of the current understanding of this phenomenon. Since the southern and northern parts of the WIS were probably not connected during the late Albian time (Fig. 8A) (Williams and Stelck, 1975; Cobban et al., 1994; Roberts and Kirschbaum, 1995; Blakey, 2013), it can be argued that the Boreal water most likely played very limited or no role in the oxygenation of the Comanche Shelf/southern parts of WIS during the OAE1d time. This argument challenges the reliance on the mixing model between the Tethyan and Boreal water masses to explain the decoupling between CIE and the deposition of organic-rich mudstones in the WIS, at least for the OAE1d time. More data covering the OAE1d interval from the WIS and GOM are still needed to examine whether the bottom-water oxygenation was sourced from the Tethyan region or was caused by another paleoceanographic mechanism (e.g., localized upwelling, reduced nutrient supply leading to lower primary productivity, or transient cooling increasing oxygen solubility, among others) that has yet to be discovered.

### 5.3. Role of the ancient Lower Cretaceous reef margins on the OAE1d expression on the Comanche Shelf and GOM

Both the Aptian Sligo and Albian Stuart City rudist-dominated reef margins in the northwestern GOM have long been recognized as northeast-southwest trending bathymetric reliefs, separating the Comanche Shelf from the GOM (Bebout, 1974; Bebout and Loucks, 1974; Winker and Buffler, 1988; Scott, 1990; Waite et al., 2007; Waite, 2009; Phelps et al., 2014). Some studies have suggested a role, at least, for the Albian Stuart City margin on the character of OAE2 near the

transition from the Comanche Shelf to the deeper GOM, indicating prevailing anoxic conditions downdip from the paleo-Stuart margin compared to oxygenated settings dominating the up-dip areas (Lowery et al., 2014; Alnahwi et al., 2018).

Scott et al. (2020) hypothesized that the OAE1d expression on the Comanche Shelf and across the GOM would show a pattern similar to that reported for the OAE 2 by Lowery et al. (2014) and Alnahwi et al. (2018) (Fig. 8C), although they provided no supporting data for this claim. Scott et al. (2020) postulated that the paleo-Stuart City margin would act as a bathymetric sill, limiting the circulation of water masses between the deep oceanic anoxic water and the shallow oxic water of the Comanche Shelf during the OAE1d time.

The data from Howell-1, located downdip from the Stuart City margin, presents an excellent opportunity to test the hypothesis proposed by Scott et al. (2020). Based on the sedimentological and TOC data from Howell-1, oxic conditions prevailed in the areas downdip from the paleo-Stuart City margin during OAE1d (Fig. 8D). This trend invalidates the hypothesis advanced by Scott et al. (2020) and suggests that the behavior of OAE1d differs significantly from that of OAE2 in the regions downdip from the paleo-Stuart City margin.

## 6. Conclusions

This study documents, for the first time, the globally mapped late Albian-early Cenomanian  $\delta^{13}\text{C}$  isotopic excursions in the WIS and GOM. The presented age-constrained, high-resolution  $\delta^{13}\text{C}_{\text{org}}$  data from the Comanche Shelf of Texas unveiled four positive carbon isotopic excursions (CIEs) with magnitudes ranging from 0.8 to 1.5 %. These excursions are comparable in magnitude and trend to the OAE1d-CIE and the other three CIEs documented globally within this interval.

The sedimentological and TOC data (<0.35 wt%) from this study indicate oxic conditions during the OAE1d interval across parts of the Comanche Shelf and southern WIS, suggesting that some local factors may have isolated this region from the broader global trend. Furthermore, unlike the trend observed within the OAE2, the areas downdip from the paleo-Stuart City margin remained oxygenated during the OAE1d time.

By documenting the late Albian-early Cenomanian  $\delta^{13}\text{C}$  isotopic excursions in the WIS and GOM, this study establishes chemostratigraphic markers for global correlations, connecting North America with equivalent intervals from the adjacent Pacific and Atlantic oceans as well as various basins worldwide.

## CRediT authorship contribution statement

**Abdulkarim Al-Hussaini:** Writing – review & editing, Writing – original draft, Visualization, Methodology, Investigation, Formal analysis, Data curation, Conceptualization. **Charles Kerans:** Writing – review & editing, Supervision, Methodology, Conceptualization. **Cornel Olariu:** Writing – review & editing, Supervision, Conceptualization. **James Pospichal:** Writing – review & editing, Formal analysis.

## Declaration of competing interest

The authors declare the following financial interests/personal relationships which may be considered as potential competing interests:

Abdulkarim Al-Hussaini reports financial support was provided by American Association of Petroleum Geologists. If there are other authors, they declare that they have no known competing financial interests or personal relationships that could have appeared to influence the work reported in this paper.

## Acknowledgment

Abdulkarim thanks the AAPG for partially funding this study and the Bureau of Economic Geology (BEG) staff for their assistance with the

Howell-1 core. He also extends his appreciation to Ardiansyah Koeshidayatullah, Khalid Al-Ramadan, Mahmoud Alnazghah, and Mohammed Fallatah for their valuable critiques and reviews, as well as to Camilo Polo and Mohammed Al-Zahrani for their help in defining key trace fossil assemblages. The authors express gratitude to Mitch Covington at BugWare, Inc. for providing the microscope and camera used in nannofossil analysis.

## Appendix A. Supplementary data

Supplementary data to this article can be found online at <https://doi.org/10.1016/j.palaeo.2025.113261>.

## Data availability

The authors confirm that all data necessary for supporting the scientific findings of this paper have been provided.

## References

- Allan, J., Matthews, R.K., 1990. Isotope signatures associated with early meteoric diagenesis. *Carbon. Diagen.* 197–217.
- Alnahwi, A., Loucks, R.G., Ruppel, S.C., Scott, R.W., Tribouillard, N., 2018. Dip-related changes in stratigraphic architecture and associated sedimentological and geochemical variability in the Upper cretaceous Eagle Ford Group in South Texas. *AAPG Bull.* 102 (12), 2537–2568.
- Alnazghah, M., Koeshidayatullah, A., Al-Hussaini, A., Amao, A., Song, H., Al-Ramadan, K., 2022. Evidence for the early Toarcian Carbon Isotope Excursion (T-CIE) from the shallow marine siliciclastic red beds of Arabia. *Sci. Rep.* 12 (1), 18124.
- Alves, C.F., de Oliveira Lima, F.H., Mendonça Filho, J.G., 2024. *Nannoconus fragilis* and *Nannoconus quadriangulus*: Taxonomic and biostratigraphic revision from Aptian-Albian sections in Brazil. *J. Nannoplank. Res.* 42 (1), 13–35.
- Arthur, M.A., Schlanger, S.O., 1979. Cretaceous “oceanic anoxic events” as causal factors in development of reef-reservoir giant oil fields. *AAPG bulletin* 63 (6), 870–885.
- Bąk, K., Szram, E., Zielińska, M., Misz-Kennan, M., Fabiańska, M., Bąk, M., Górný, Z., 2023. Organic matter variations in the deep marginal basin of the Western Tethys and links to various environments in isotopic Albian-Cenomanian Boundary Interval. *Int. J. Coal Geol.* 266, 104181.
- Bebout, D.G., 1974. Lower Cretaceous Stuart City Shelf Margin of South Texas: Its Depositional and Diagenetic Environments and their Relationship to Porosity, 24. Gulf Coast Association of Geological Societies Transactions, pp. 138–159.
- Bebout, D.G., Loucks, R.G., 1974. Stuart City trend, Lower Cretaceous, south Texas : a carbonate shelf-margin model for hydrocarbon exploration. In: Report of Investigations - Bureau of Economic Geology, University of Texas at Austin no. 78. Bureau of Economic Geology, University of Texas at Austin. Report of Investigations 78., Austin, p. 80.
- Blakey, R., 2013. North American Paleogeography. Colorado Plateau Geosystems Inc.
- Bornemann, A., Pross, J., Reichelt, K., Herrle, J.O., Hemleben, C., Mutterlose, J., 2005. Reconstruction of short-term palaeoceanographic changes during the formation of the late Albian ‘Niveau Breistroffer’ black shales (Oceanic Anoxic Event 1d, SE France). *J. Geol. Soc. London* 162 (4), 623–639.
- Bornemann, A., Erbacher, J., Heldt, M., Kollaske, T., Wilmsen, M., Lübke, N., Huck, S., Voßmar, M., Wonik, T., 2017. The Albian-Cenomanian transition and Oceanic Anoxic Event 1d—an example from the boreal realm. *Sedimentology* 64 (1), 44–65.
- Bornemann, A., Erbacher, J., Blumenberg, M., Voigt, S., 2023. A first high-resolution carbon isotope stratigraphy from the Boreal (NW Germany) for the Berriasian to Coniacian interval—implications for the timing of the Aptian-Albian boundary. *Front. Earth Sci.* 11, 1173319.
- Bown, P.R., 1998. Calcareous Nannofossil Biostratigraphy. British Micropalaeontological Society publication series, Chapman & Hall, London, vii, p. 314.
- Bown, P.R., 2005. Early to Mid-Cretaceous Calcareous Nannoplankton from the Northwest Pacific Ocean, Leg 198, Shatsky Rise, Proceedings of the Ocean Drilling Program. Scientific Results. Ocean Drilling Program College Station, TX, pp. 1–82.
- Bown, P.R., Rutledge, D., Crux, J., Gallagher, L., 1998. Lower cretaceous. In: Bown, P.R. (Ed.), *Calcareous Nannofossil Biostratigraphy*. Chapman & Hall, London, pp. 86–131.
- Bréhéret, J.G., 1988. Episodes de sédimentation riche en matière organique dans les marnes bleues d’âge aptien et albien de la partie pélagique du bassin vocontien. *Bull. Soc. Géol. France* 4 (2), 349–356.
- Bréhéret, J.-G., 1997. L’Aptien et l’Albien de la fosse vocontienne (des bordures au bassin): Évolution de la sédimentation et enseignements sur les événements anoxiques. Université François Rabelais-Tours.
- Breistroffer, M., 1937. Sur les niveaux fossilifères de l’Albien dans la fosse vocontienne (Drôme, Hautes-Alpes et Basses-Alpes). *Comptes Rendus de l’Académie des Sciences*, pp. 1492–1493.
- Buffler, R.T., 1991. Early evolution of the Gulf of Mexico basin. In: Goldthwaite, D. (Ed.), *An Introduction to Central Gulf Coast Geology*: New Orleans Geological Society, Louisiana, pp. 1–15.
- Burnett, J., 1998. Upper cretaceous. In: Bown, P.R. (Ed.), *Calcareous Nannofossil Biostratigraphy*. Chapman & Hall, London, pp. 132–199.
- Cobban, W., Merewether, E., Fouch, T., Obradovich, J., 1994. Some Cretaceous Shorelines in the Western Interior of the United States. Mesozoic Systems of the Rocky Mountain Region. *SEPM Rocky Mountain Section*, pp. 393–414.
- Cramer, B., Jarvis, I., 2020. Carbon isotope stratigraphy, Geologic time scale 2020. Elsevier 309–343.
- Denne, R.A., Breyer, J.A., Kosanke, T.H., Spaw, J.M., Callender, A.D., Hinote, R.E., Karimina, M., Tur, N., Kita, Z., Lees, J.A., Rowe, H., 2016. Biostatigraphic and Geochemical Constraints on the Stratigraphy and Depositional Environments of the Eagle Ford and Woodbine groups of Texas. In: Breyer, J. (Ed.), *The Eagle Ford Shale, A Renaissance in U.S. Oil Production*. AAPG Memoir, vol. 110, pp. 1–86.
- Dickson, J., Coleman, M., 1990. Changes in carbon and oxygen isotope composition during limestone diagenesis. *Carbon. Diagen.* 259–270.
- Elderbak, K., Leckie, R.M., 2016. Paleocirculation and foraminiferal assemblages of the Cenomanian-Turonian Bridge Creek Limestone bedding couplets: Productivity vs. dilution during OAE2. *Cretaceous Res.* 60, 52–77.
- Elderbak, K., Leckie, R.M., Tibert, N.E., 2014. Paleoenvironmental and paleoceanographic changes across the Cenomanian-Turonian Boundary Event (Oceanic Anoxic Event 2) as indicated by foraminiferal assemblages from the eastern margin of the Cretaceous Western Interior Sea. *Palaeogeogr. Palaeoclimatol. Palaeoecol.* 413, 29–48.
- Eldrett, J.S., Minisini, D., Bergman, S.C., 2014. Decoupling of the carbon cycle during Ocean Anoxic Event 2. *Geology* 42 (7), 567–570.
- Eldrett, J.S., Dodsworth, P., Bergman, S.C., Wright, M., Minisini, D., 2017. Water-mass evolution in the cretaceous western interior seaway of North America and equatorial Atlantic. *Clim. Past* 13 (7), 855–878.
- Erba, E., 2004. Calcareous nannofossils and Mesozoic oceanic anoxic events. *Mar. Micropaleontol.* 52 (1–4), 85–106.
- Ewing, T.E., 1991. Structural framework. In: Salvador, A. (Ed.), *The Gulf of Mexico Basin*. Geological Society of America.
- Gale, A.S., Kennedy, W.J., Burnett, J., Caron, M., Kidd, B., 1996. The Late Albian to Early Cenomanian succession at Mont Risou near Rosans (Drôme, SE France): an integrated study (ammonites, inocerams, planktonic foraminifera, nannofossils, oxygen and carbon isotopes). *Cretaceous Res.* 17 (5), 515–606.
- Gale, A., Mutterlose, J., Batenburg, S., Gradstein, F., Agterberg, F., Ogg, J., Petrizzo, M., 2020. The cretaceous period, Geologic time scale 2020. Elsevier 1023–1086.
- Gale, A.S., Rashall, J.M., Kennedy, W.J., Holterhoff, F.K., 2021. The microcrinoid taxonomy, biostratigraphy and correlation of the upper Fredericksburg and lower Washita groups (cretaceous, middle Albian to lower Cenomanian) of northern Texas and southern Oklahoma, USA. *Acta Geol. Pol.* 71 (1), 1–52.
- Gambacorta, G., Jenkyns, H., Russo, F., Tsikos, H., Wilson, P., Faucher, G., Erba, E., 2015. Carbon-and oxygen-isotope records of mid-cretaceous Tethyan pelagic sequences from the Umbria-Märche and Belluno Basins (Italy). *Newsl. Stratigr.* 48 (3), 299–323.
- Gambacorta, G., Bottini, C., Brumsack, H.-J., Schnetger, B., Erba, E., 2020. Major and trace element characterization of Oceanic Anoxic Event 1d (OAE 1d): insight from the Umbria-Märche Basin, Central Italy. *Chem. Geol.* 557, 119834.
- Ge, Y., Han, Z., Algeo, T.J., Kemp, D.B., Wu, L., 2024. Heterogeneous marine response during the Toarcian Oceanic Anoxic Event (TOAE): the potential role of storminess. *Global Planet. Change* 242, 104533.
- Gradstein, F.M., Ogg, J.G., 2020. The chronostratigraphic scale, Geologic time scale 2020. Elsevier 21–32.
- Gröcke, D.R., Ludvigson, G.A., Witzke, B.L., Robinson, S.A., Joeckel, R., Ufnar, D.F., Ravn, R.L., 2006. Recognizing the Albian-Cenomanian (OAE1d) sequence boundary using plant carbon isotopes: Dakota formation, Western Interior Basin, USA. *Geology* 34 (3), 193–196.
- Gyawali, B.R., Nishi, H., Takashima, R., Herrle, J.O., Takayanagi, H., Latil, J.-L., Iryu, Y., 2017. Upper Albian–upper Turonian calcareous nannofossil biostratigraphy and chemostratigraphy in the Vocontian Basin, southeastern France. *Newslett. Stratigr.* 50 (2), 111–139.
- Hallock, P., Schlager, W., 1986. Nutrient excess and the demise of coral reefs and carbonate platforms. *Palaeos* 389–398.
- Hennhofer, D., Al Suwaidi, A., Bottini, C., Helja, E., Steuber, T., 2019. The Albian to Turonian carbon isotope record from the Shilaif Basin (United Arab Emirates) and its regional and intercontinental correlation. *Sedimentology* 66 (2), 536–555.
- Herlambang, A., Koeshidayatullah, A.I., Al-Hussaini, A., Amao, A.O., Alnazghah, M.H., Fallatah, M., Algheryafi, H., Al-Ramadan, K.A., 2023. Expression of the Toarcian Oceanic Anoxic Event in the mixed siliciclastic-carbonate system of the Arabian Plate: Insights from rare-earth element geochemistry and statistical analysis. *Sediment. Geol.* 452, 106393.
- Herrle, J.O., Köbler, P., Friedrich, O., Erlenkeuser, H., Hemleben, C., 2004. High-resolution carbon isotope records of the Aptian to lower Albian from SE France and the Mazagan Plateau (DSDP Site 545): a stratigraphic tool for paleoceanographic and paleobiologic reconstruction. *Earth Planet. Sci. Lett.* 218 (1–2), 149–161.
- Herrle, J.O., Schröder-Adams, C.J., Davis, W., Pugh, A.T., Galloway, J.M., Fath, J., 2015. Mid-cretaceous High Arctic stratigraphy, climate, and oceanic anoxic events. *Geology* 43 (5), 403–406.
- Jarvis, I., Gale, A.S., Jenkyns, H.C., Pearce, M.A., 2006. Secular variation in Late Cretaceous carbon isotopes: a new δ<sup>13</sup>C carbonate reference curve for the Cenomanian–Campanian (99.6–70.6 Ma). *Geol. Mag.* 143 (5), 561–608.
- Jarvis, I., Lignum, J.S., Gröcke, D.R., Jenkyns, H.C., Pearce, M.A., 2011. Black shale deposition, atmospheric CO<sub>2</sub> drawdown, and cooling during the Cenomanian–Turonian Oceanic Anoxic Event. *Paleoceanography* 26 (3).
- Jenkyns, H.C., 2010. Geochemistry of oceanic anoxic events. *Geochem. Geophys. Geosyst.* 11 (3).

- Jenkyns, H., Gale, A., Corfield, R., 1994. Carbon-and oxygen-isotope stratigraphy of the English Chalk and Italian Scaglia and its palaeoclimatic significance. *Geol. Mag.* 131 (1), 1–34.
- Jeremiah, J., 1996. A proposed Albian to lower Cenomanian nannofossil biozonation for England and the North Sea Basin. *J. Micropalaeontol.* 15 (2), 97–129.
- Kanungo, S., Bown, P., Gale, A., 2021. Cretaceous (Albian-Turonian) calcareous nannofossil biostratigraphy of the onshore Cauvery Basin, southeastern India. *Cretaceous Res.* 118, 104644.
- Kennedy, W., Gale, A., Lees, J., Caron, M., 2004. The global boundary stratotype section and point (GSSP) for the base of the Cenomanian Stage, Mont Risou, Hautes-Alpes, France. *Episod. J. Int. Geosci.* 27 (1), 21–32.
- Kerans, C., 2002. Styles of rudist buildup development along the northern margin of the Maverick Basin, Pecos River Canyon, Southwest Texas. *Gulf Coast Assoc. Geol. Soc. Trans.* 52, 501–516.
- Leckie, R.M., 1985. Foraminifera of the Cenomanian-Turonian boundary interval, greenhorn formation, Rock Canyon Anticline, Pueblo, Colorado. In: Pratt, L.M., Kauffman, E.G., Zelt, F.B. (Eds.), *Fine-Grained Deposits and Biofacies of the Cretaceous Western Interior Seaway: Evidence of Cyclic Sedimentary Processes*. SEPM Society for Sedimentary Geology (pp. 0).
- Leckie, R.M., Yuretich, R.F., West, O.L.O., Finkelstein, D., Schmidt, M., 1998. Paleoceanography of the Southwestern Western Interior Sea during the Time of the Cenomanian-Turonian Boundary (Late Cretaceous). In: Dean, W.E., Arthur, M.A. (Eds.), *Stratigraphy and Paleoenvironments of the Cretaceous Western Interior Seaway*, USA. SEPM Society for Sedimentary Geology (pp. 0).
- Lowery, C.M., Corbett, M.J., Leckie, R.M., Watkins, D., Romero, A.M., Pramudito, A., 2014. Foraminiferal and nannofossil paleoecology and paleoceanography of the Cenomanian-Turonian Eagle Ford Shale of southern Texas. *Palaeogeogr. Palaeoclimatol. Palaeoecol.* 413, 49–65.
- Lowery, C.M., Leckie, R.M., Bryant, R., Elderbak, K., Parker, A., Polyak, D.E., Schmidt, M., Snoeyenbos-West, O., Sterzinar, E., 2018. The late cretaceous Western Interior Seaway as a model for oxygenation change in epicontinental restricted basins. *Earth Sci. Rev.* 177, 545–564.
- Mancini, E.A., 1979. Late Albian and early Cenomanian Grayson ammonite biostratigraphy in north-Central Texas. *J. Paleo.* 1013–1022.
- Mitchell, S., Paul, C., Gale, A., 1996. Carbon isotopes and sequence stratigraphy. *Geol. Soc. Lond. Spec. Publ.* 104 (1), 11–24.
- Navarro-Ramirez, J.P., Bodin, S., Heimhofer, U., Immenhauser, A., 2015. Record of Albian to early Cenomanian environmental perturbation in the eastern sub-equatorial Pacific. *Palaeogeogr. Palaeoclimatol. Palaeoecol.* 423, 122–137.
- Navarro-Ramirez, J., Bodin, S., Consorti, L., Immenhauser, A., 2017. Response of western South American epeiric-neritic ecosystem to middle cretaceous Oceanic Anoxic events. *Cretaceous Res.* 75, 61–80.
- Navidtalab, A., Heimhofer, U., Huck, S., Omidvar, M., Rahimpour-Bonab, H., Aharipour, R., Shakeri, A., 2019. Biochemostratigraphy of an upper Albian–Turonian succession from the southeastern Neo-Tethys margin, SW Iran. *Palaeogeogr. Palaeoclimatol. Palaeoecol.* 533, 109255.
- Nederbragt, A.J., Fiorentino, A., Kłosowska, B., 2001. Quantitative analysis of calcareous microfossils across the Albian–Cenomanian boundary oceanic anoxic event at DSDP Site 547 (North Atlantic). *Palaeogeogr. Palaeoclimatol. Palaeoecol.* 166 (3–4), 401–421.
- Perch-Nielsen, K., 1985. Mesozoic calcareous nannofossil. In: Bolli, H.M., Saunders, J.B., Perch-Nielsen, K. (Eds.), *Plankton Stratigraphy*. Cambridge University, New York, pp. 329–426.
- Petrizzi, M.R., Huber, B.T., Wilson, P.A., MacLeod, K.G., 2008. Late Albian paleoceanography of the western subtropical North Atlantic. *Paleoceanography* 23 (1).
- Phelps, R.M., Kerans, C., Loucks, R.G., Da Gama, R.O., Jeremiah, J., Hull, D., 2014. Oceanographic and eustatic control of carbonate platform evolution and sequence stratigraphy on the cretaceous (Valanginian–Campanian) passive margin, northern Gulf of Mexico. *Sedimentology* 61 (2), 461–496.
- Phelps, R.M., Kerans, C., Da-Gama, R.O., Jeremiah, J., Hull, D., Loucks, R.G., 2015. Response and recovery of the Comanche carbonate platform surrounding multiple cretaceous oceanic anoxic events, northern Gulf of Mexico. *Cretac. Res.* 54, 117–144.
- Philip, J., Airaud-Crumiere, C., 1991. The demise of the rudist-bearing carbonate platforms at the Cenomanian/Turonian boundary: a global control. *Coral Reefs* 10 (2), 115–125.
- Pratt, L.M., Threlkeld, C.N., 1984. Stratigraphic Significance of  $^{13}\text{C}/^{12}\text{C}$  Ratios in Mid-Cretaceous Rocks of the Western Interior, U.S.A., The Mesozoic of Middle North America: A Selection of Papers from the Symposium on the Mesozoic of Middle North America. Canadian Society of Petroleum Geologists, Calgary, Alberta, Canada, pp. 305–312.
- Richey, J.D., Upchurch, G.R., Montañez, I.P., Lomax, B.H., Suarez, M.B., Crout, N.M., Joeckel, R., Ludvigson, G.A., Smith, J.J., 2018. Changes in CO<sub>2</sub> during Ocean Anoxic Event 1d indicate similarities to other carbon cycle perturbations. *Earth Planet. Sci. Lett.* 491, 172–182.
- Roberts, L.N.R., Kirschbaum, M.A., 1995. Paleogeography and the Late Cretaceous of the Western Interior of Middle North America; Coal Distribution and Sediment Accumulation. U.S. Geological Survey (Professional Paper 1561).
- Robinson, S.A., Clarke, L.J., Nederbragt, A., Wood, I.G., 2008. Mid-cretaceous oceanic anoxic events in the Pacific Ocean revealed by carbon-isotope stratigraphy of the Calera Limestone, California, USA. *Geol. Soc. Am. Bull.* 120 (11–12), 1416–1426.
- Rodríguez-Cuicas, M.-E., Montero-Serrano, J.-C., Garbán, G., 2019. Paleoenvironmental changes during the late Albian oceanic anoxic event 1d: an example from the Capache Formation, southwestern Venezuela. *Palaeogeogr. Palaeoclimatol. Palaeoecol.* 521, 10–29.
- Rodríguez-Cuicas, M.-E., Montero-Serrano, J.-C., Garbán, G., 2020. Geochemical and mineralogical records of late Albian oceanic anoxic event 1d (OAE-1d) in the La Grita Member (southwestern Venezuela): Implications for weathering and provenance. *J. South Am. Earth Sci.* 97, 102408.
- Rose, P., 1972. Edwards Group, Surface and Subsurface, Central Texas: Bureau of Economic Geology, 74. University of Texas at Austin Report of Investigations, p. 198.
- Salvador, A., 1991. The Gulf of Mexico Basin. Geological Society of America, Boulder, Colo., ix, *Geology of North America*, p. 568.
- Schlager, W., 1981. The paradox of drowned reefs and carbonate platforms. *Geol. Soc. Am. Bull.* 92 (4), 197–211.
- Schlanger, S., Jenkyns, H., 1976. Cretaceous oceanic anoxic events: causes and consequences. *Geol. Mijnb.* 55 (3–4).
- Schröder-Adams, C.J., Herrele, J.O., Tu, Q., 2012. Albian to Santonian carbon isotope excursions and faunal extinctions in the Canadian Western Interior Sea: Recognition of eustatic sea-level controls on a forebulge setting. *Sedimentary Geology* 281, 50–58.
- Scott, R.W., 1990. Models and Stratigraphy of Mid-Cretaceous Reef Communities. SEPM Society for Sedimentary Geology, Gulf of Mexico.
- Scott, R.W., Benson, D.G., Morin, R.W., Shaffer, B.L., Oboh-Ikuenobe, F.E., 2003. Integrated Albian-Lower Cenomanian chronostratigraphy standard, Trinity River section, Texas, US Gulf Coast Cretaceous stratigraphy and paleoecology: Gulf Coast Section, Society of Economic Paleontologists and Mineralogists, Bob F. Perkins Memorial Conference, pp. 277–334.
- Scott, R.W., Formolo, M., Rush, N., Owens, J.D., Oboh-Ikuenobe, F., 2013. Upper Albian OAE 1d event in the Chihuahua Trough, New Mexico, USA. *Cretaceous Res.* 46, 136–150.
- Scott, R.W., Oboh-Ikuenobe, F.E., Benson Jr., D.G., Holbrook, J.M., Alnahwi, A., 2018. Cenomanian-Turonian flooding cycles: US Gulf Coast and western interior. *Cretaceous Res.* 89, 191–210.
- Scott, R., Campbell, W., Diehl, B., Edwards, W., Altintas, D.G., Harlton, K., Hojnacki, R., Lai, X., Porter, A., Rush, N., 2019. Regional upper Albian-lower Cenomanian sequence boundaries, Texas Comanche shelf: is timing related to oceanic tectonics? *Cretaceous Res.* 98, 335–362.
- Scott, R.W., Rush, N., Hojnacki, R., Campbell, W., Wang, Y., Lai, X., 2020. Albian (lower cretaceous) carbon isotope chemozones, Texas Comanche Shelf and Mexican Chihuahua Trough: Implications for OAEs. *Cretaceous Res.* 112, 104453.
- Sneden, J.W., Galloway, W.E., 2019. The Gulf of Mexico Sedimentary Basin: Depositional Evolution and Petroleum Applications. Cambridge University Press.
- Taylor, A., Goldring, R., 1993. Description and analysis of bioturbation and ichnofabric. *J. Geol. Soc. London* 150 (1), 141–148.
- Vahrenkamp, V.C., 2013. Carbon-isotope signatures of Albian to Cenomanian (cretaceous) shelf carbonates of the Natih Formation, Sultanate of Oman. *GeoArabia* 18 (3), 65–82.
- Waite, L.E., 2009. Edwards (Stuart City) Shelf Margin of South Texas: New Data. Tulsa Geological Society, Tulsa, Oklahoma, USA, New Concepts, p. 9.
- Waite, L.E., Scott, R.W., Kerans, C., 2007. Middle Albian age of the regional dense marker bed of the Edwards Group, Pawnee Field, south-Central Texas. *Gulf Coast Assoc. Geol. Soc. Trans.* 57, 759–774.
- Watkins, D.K., Cooper, M.J., Wilson, P.A., 2005. Calcareous nannoplankton response to late Albian oceanic anoxic event 1d in the western North Atlantic. *Paleoceanography* 20 (2).
- Williams, G., Stelck, C.R., 1975. Speculations on the Cretaceous palaeogeography of North America. In: Cladwell, W.G.E. (Ed.), *The Cretaceous System in the Western Interior of North America*. Geological Association of Canada, pp. 1–20.
- Wilson, P.A., Norris, R.D., 2001. Warm tropical ocean surface and global anoxia during the mid-cretaceous period. *Nature* 412 (6845), 425–429.
- Winker, C.D., Buffler, R.T., 1988. Paleoceanographic evolution of early deep-water Gulf of Mexico and margins, Jurassic to Middle cretaceous (Comanchean). *AAPG Bull.* 72 (3), 318–346.
- Wohlwend, S., Hart, M., Weissert, H., 2016. Chemostratigraphy of the Upper Albian to mid-Turonian Natih Formation (Oman)—how authigenic carbonate changes a global pattern. *Depositional Rec.* 2 (1), 97–117.
- Yao, H., Chen, X., Melinte-Dobrescu, M.C., Wu, H., Liang, H., Weissert, H., 2018. Biostratigraphy, carbon isotopes and cyclostratigraphy of the Albian-Cenomanian transition and Oceanic Anoxic Event 1d in southern Tibet. *Palaeogeogr. Palaeoclimatol. Palaeoecol.* 499, 45–55.